PTP1B antisense oligonucleotide lowers PTP1B protein, normalizes blood glucose, and improves insulin sensitivity in diabetic mice

Bradley A. Zinker*[†‡], Cristina M. Rondinone*[†], James M. Trevillyan*[†], Rebecca J. Gum*, Jill E. Clampit*, Jeffrey F. Waring*, Nancy Xie*, Denise Wilcox*, Peer Jacobson*, Leigh Frost*, Paul E. Kroeger*, Regina M. Reilly*, Sandra Koterski*, Terry J. Opgenorth*, Roger G. Ulrich*[§], Seth Crosby*[¶], Madeline Butler[‖], Susan F. Murray[‖], Robert A. McKay[‖], Sanjay Bhanot[‖], Brett P. Monia[‖], and Michael R. Jirousek*[,**]

*Abbott Laboratories, 100 Abbott Park Road, Abbott Park, IL 60064-3500; and [‖]Isis Pharmaceuticals, 2292 Faraday Avenue, Carlsbad, CA 92008

The role of protein-tyrosine phosphatase 1B (PTP1B) in diabetes was investigated using an antisense oligonucleotide in *ob*/*ob* and *db*/*db* mice. PTP1B antisense oligonucleotide treatment normalized plasma glucose levels, postprandial glucose excursion, and HbA$_{1C}$. Hyperinsulinemia was also reduced with improved insulin sensitivity. PTP1B protein and mRNA were reduced in liver and fat with no effect in skeletal muscle. Insulin signaling proteins, insulin receptor substrate 2 and phosphatidylinositol 3 (PI3)-kinase regulatory subunit p50α, were increased and PI3-kinase p85α expression was decreased in liver and fat. These changes in protein expression correlated with increased insulin-stimulated protein kinase B phosphorylation. The expression of liver gluconeogenic enzymes, phosphoenolpyruvate carboxykinase, and fructose-1,6-bisphosphatase was also down-regulated. These findings suggest that PTP1B modulates insulin signaling in liver and fat, and that therapeutic modalities targeting PTP1B inhibition may have clinical benefit in type 2 diabetes.

Insulin resistance in peripheral tissues including liver, fat, and skeletal muscle characterizes type 2 diabetes. Insulin resistance is associated with other pathological conditions including obesity, hypertriglyceridemia, and hypertension (1). The molecular mechanism of insulin resistance is not well understood but does not appear to involve structural defects in the insulin receptor (IR) (2). The molecular basis for insulin resistance appears to involve an early process in IR signal transduction (3, 4).

Insulin signaling is initiated when insulin binds to the extracellular α-subunits of the $\alpha_2\beta_2$ heterotetrameric insulin receptor. Insulin binding to the IR induces activation of the kinase domain and autophosphorylation of at least six tyrosine residues within three distinct domains of the β-subunit (5). Autophosphorylation of tyrosine residues 1146, 1150, and 1151 in the kinase domain of the β-subunit activates the insulin receptor kinase and causes the phosphorylation of other protein substrates, including IR substrates (IRS-1 to -4) and other adapter proteins (Gab1 and Shc) that mediate the biological effects of insulin (6–9).

Protein-tyrosine phosphatase 1B (PTP1B) negatively regulates IR and IRS-1 phosphorylation (10–12). Mice that have the PTP1B gene ablated have increased insulin sensitivity with resistance to weight gain on a high-fat diet (13, 14). However, the role of PTP1B in the diabetic state has not been elucidated. To determine the effect of reducing PTP1B protein level in the diabetic state and subsequent effect on insulin signaling, an antisense oligonucleotide (ASO) was optimized to selectively bind to PTP1B mRNA and reduce PTP1B protein expression (15, 16). PTP1B ASO was demonstrated to improve glycemic control in obese and insulin resistant diabetic *ob*/*ob* and *db*/*db* mice. In *ob*/*ob* mice, PTP1B ASO was also demonstrated to affect the expression of insulin signaling proteins in liver and fat and to improve insulin sensitivity in liver. These data suggest that PTP1B modulates insulin signaling in liver and fat and that therapeutic modalities targeting PTP1B inhibition may have clinical benefit in type 2 diabetes.

Experimental Procedures

Selection of PTP1B ASO. Rapid throughput screens for identifying ASO inhibitors selective against PTP1B were performed with 20-base chimeric ASOs where the first five bases and last five bases have a 2′-*O*-(2-methoxy)-ethyl (2′-MOE) modification. The 2′-MOE modification increases binding affinity to complementary RNA sequences and increases resistance to nucleases (17). The ASO oligonucleotides have a phosphorothioate backbone and use an RNase H-dependent mechanism for activity. Initial screens were conducted against rat PTP1B and ten ASOs were identified as hits, all of which targeted the same binding site within the coding region of the PTP1B mRNA. Subsequently, a series of *in vitro* characterization experiments were performed in primary rat and mouse hepatocytes, in which ISIS-113715 was consistently identified to be the most potent and specific oligonucleotide in reducing PTP1B mRNA levels. ISIS-113715 hybridizes to PTP1B mRNA at nucleotides 861–880 in the coding sequence. A universal control (UC) oligonucleotide pool (ISIS-29848) was synthesized as a mixture of A (adenine), G (guanosine), T (thymine), and C (cytosine) bases so that the resulting preparation contains an equimolar mixture of all 4^{19} possible oligonucleotides. The oligonucleotide chemistry of ISIS-29848 was identical to that of ISIS-113715.

Animal Care and Treatments. *ob*/*ob* and *db*/*db* mice and their lean littermates of 6–7 weeks of age (The Jackson Laboratory) were acclimated to the animal research facilities for 5 days. The following investigations were conducted in accordance with each institutions IACUC guidelines. Animals were housed five per cage *ob*/*ob* (C57BL/6J- Lep^{ob}/Lep^{ob}), two per cage lean *ob*/+ littermates (C57BL/6J-Lep^{ob}/+), four per cage *db*/*db* (C57BLKS/J-*m*Lepr^{db}/Lepr^{db}), and two per cage lean *db*/+ littermates (C57BLKS/J-*m*Lepr^{db}/+) and maintained on mouse

MEDICAL SCIENCES

chow (*ob/ob* Labdiets #5015, St. Louis; *db/db* Harlan-Teklad rodent diet #8604 Madison, WI; 26% fat calories) *ad libitum*.

After acclimation the *ob/ob* and lean mice were weighed and tail snip glucose levels were determined by the glucose oxidase method (Precision G glucose meter, Abbott Laboratories, North Chicago). The animals were randomized to the various treatment groups based on plasma glucose levels and body weight. Baseline plasma insulin samples were taken from a subset of the animals representing each treatment group once randomized (*n* = 10 *ob/ob* and *n* = 10 lean *ob/+* littermates; ELISA, ALPCO Diagnostics, Windham, NH). Three separate experiments were performed with PTP1B ASOs. Treatment groups were as follows. Experiment 1: *ob/ob* and *ob/+* mice treated with PTP1B ASO at 50 mg/kg (*n* = 9) for 3 weeks; experiment 2: *ob/ob* and *ob/+* mice treated with PTP1B ASO at 25, 2.5, or 0.25 mg/kg or saline (*n* = 10 per treatment) for 6 weeks; experiment 3: *db/db* and *db/+* mice treated with PTP1B ASO at 50, 25, or 10 mg/kg or saline or universal control oligonucleotide (UC) at 50 mg/kg for 4 weeks (*n* = 8 per treatment glucose and *n* = 3 per treatment for all other parameters). Mice were dosed i.p. either twice per week (*ob/ob* and *ob/+*) or once per week (*db/db* and *db/+*). The ASO were weighed and resuspended in saline at a concentration of 25 mg/ml. The suspension was vortexed and allowed to sit at room temperature for 15 min and was then filtered through a syringe filter (0.2 μm; Gelman Acrodisc). The filtrate (2 μl) was diluted in 1 ml of H$_2$O and OD read at 260 nM. The formula used to calculate the concentration was as follows: (OD · dilution factor · molecular weight)/(extinction coefficient · 1,000) = concentration in mg/ml. The stock was diluted to the desired concentration for injection in sterile saline and frozen at 20°C. For subsequent use, the stock was thawed, heated to 37°C, and vortexed before using. At the end of each week tail bleed glucose and insulin (*ob/ob* and *ob/+* only) levels, as well as body weight, were determined under nonfasting conditions by 10:00 a.m. (as described above). A gross estimation of food consumption was determined in *ob/ob* mice each week as follows. Food was measured at 10:00 a.m. at the start and end of a 24-h period (same 24-h period each week), and divided by the number of mice per cage for an index of estimated 24 h food consumption per mouse. At the end of the studies, liver, epididymal fat pads, and skeletal muscle were harvested and frozen immediately in liquid nitrogen for further analysis.

Glucose and Insulin Tolerance Tests (GTT and ITT). An i.p. GTT was performed at 0.5 g/kg (50% solution of D-50 Dextrose, Abbott Laboratories, North Chicago). After a 3-h fast beginning at 6:30 a.m., a baseline 0-min sample was taken followed by an i.p. injection of glucose. Tail bleed samples were taken at 15, 30, 60, and 120 min following glucose injection. *ob/ob* and *ob/+* mice were studied after 3 or 6 weeks of treatment. The 6-week 25 mg/kg and saline control treatments underwent an i.p. ITT (2 units insulin per kg in 0.1% BSA; R-Insulin, Lilly Research Laboratories, Indianapolis). After a 5-h fast and a baseline 0-min tail bleed for glucose determination, an i.p. injection of insulin was given and additional glucose samples were taken at 15, 30, 60, and 120 min.

Insulin Challenge. In a parallel group of identically treated *ob/ob* mice, a saline or insulin challenge was administered at 0 min after an overnight fast. Insulin (2 units/kg in 0.1% BSA) or saline control was given i.p. Tissue samples from liver (0, 1, and 5 min) were taken under both saline and insulin stimulated conditions (*n* = 4 per treatment per time point). Within each challenge (saline and insulin) were subgroups of saline- or antisense-treated (25 mg/kg) mice.

Tissue Extract Preparation, Immunoprecipitation, and Immunoblotting Techniques. Tissues were sonicated (using a Branson 450 Sonifier) in lysis buffer containing 20 mM Tris·HCl (pH 7.4), 1% Triton X-100, 10% glycerol, 150 mM NaCl, 2 mM EDTA, 25 mM β-glycerophosphate, 20 mM sodium fluoride, 1 mM sodium orthovanadate, 2 mM sodium pyrophosphate, 10 μg/ml leupeptin, 1 mM benzamidine, 1 mM 4-(2-aminoethyl) benzenesulfonyl fluoride hydrochloride, and 1 mM microcystin and rocked for 40 min at 4°C. Detergent-insoluble material was sedimented by centrifugation at 12,000 × *g* for 10 min at 4°C. Cell lysate proteins (50 μg of protein) were separated by SDS/PAGE on 10% and 7.5% gels or 100 μg of protein was immunoprecipitated for 2 h with 4G10 antiphosphotyrosine antibodies (4 μg/ml; Upstate Biotechnology, Lake Placid, NY). Immune complexes were collected with protein A-Sepharose, washed, solubilized in Laemmli sample buffer, and separated by SDS/PAGE on 7.5% gels. Proteins were transferred from the gel to nitrocellulose sheets and blocked in 5% milk. The blots were probed with various primary antibodies—antiphosphotyrosine, anti-PTP1B, anti-IRS-1 (PH domain), anti-IRS-2, anti-p85 antibodies (Upstate Biotechnology, Lake Placid, NY), anti-IRβ antibody (Transduction Laboratories, San Diego), and phospho-protein kinase B (PKB) antibody (New England Biolabs)—according to the recommendations of the manufacturers. The proteins were detected by enhanced chemiluminescence with horseradish peroxidase-labeled secondary antibodies (Amersham Pharmacia). The intensity of the bands was quantitated with a laser densitometer (Molecular Dynamics).

RNA Preparation. RNA preparation was performed by grinding approximately 100 mg of liver tissue in 1 ml of TRIzol reagent and analysis was done according to the Affymetrix protocol. Briefly, the RNA from four mice in PTP1B ASO-treated or control groups was pooled using equal amounts to make a total of 20 μg of RNA. cRNA was prepared using the Superscript Choice system from GIBCO/BRL Life Technologies (no.18090-019). The protocol was followed with the exception that the primer used for the reverse transcription reaction was a modified T7 primer with 24 thymidines at the 3′ end. The sequence was 5′-GGCCAGTGAATTGTAATACGACTCACTATAGGG-AGGCGG-(T)$_{24}$-3′. Following this, labeled cRNA was synthesized according to the manufacturer's instructions from the cDNA, using the Enzo RNA Transcript Labeling Kit (no. 900182). Approximately 20 μg of cRNA was then fragmented in a solution of 40 mM Tris-acetate, pH 8.1, 100 mM KOAc, and 30 mM MgOAc at 94°C for 35 min. Labeled cRNA was hybridized to the Affymetrix GENECHIP Test2 Array to verify the quality of labeled cRNA. Following this, cRNA was hybridized to the Affymetrix MU11K A and B chip. The cRNA was hybridized overnight at 45°C. The data were analyzed using GENECHIP version 3.2 and SPOTFIRE.NET Version 5.0 (Spotfire, Somerville, MA). The microarray experiment was repeated for the 50 mg/kg treatment group by using RNA isolated a second time from the same mouse livers, and the results are an average of the two experiments.

Statistical Analysis. Statistical evaluation was performed via 1-way ANOVA and *t* tests where appropriate, using INSTAT (GraphPad, San Diego). The level of significance was $P < 0.05$ (two-sided test).

## Results and Discussion

PTP1B ASO was administered to obese, insulin-resistant *ob/ob* and *db/db* mice. Diabetic *ob/ob* mice were treated i.p. twice per week for 6 weeks in a dose-ranging study. PTP1B protein levels were reduced in liver and fat without a reduction in skeletal muscle (Fig. 1 *A–C*). In the high-dose group, hepatic PTP1B mRNA levels were also reduced (44 ± 2%, $P < 0.05$). This is
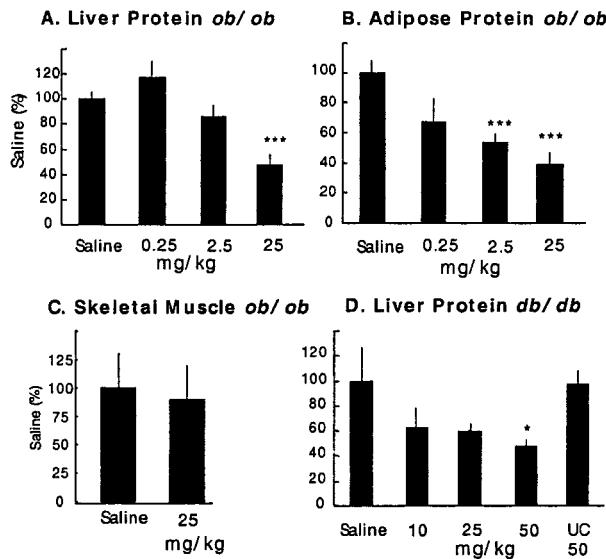
Fig. 1. PTP1B protein levels in liver (*A*), fat (*B*), and skeletal muscle (*C*) from *ob/ob* mice treated i.p. for 6 weeks twice per week with PTP1B ASO at the indicated dose. (*D*) Liver PTP1B protein levels in *db/db* mice treated i.p. once per week for 4 weeks at the indicated dose. In the *db/db* study, a UC oligonucleotide dosed at 50 mg/kg was included to control for nonspecific effects of the PTP1B ASO. Data are mean ± SE and statistics were determined as a two-tailed *t* test. *, *P* < 0. 05; ***, *P* < 0.001 (vs. saline control).

consistent with the known accumulation of ASOs into liver and fat with little penetration into muscle (18). The same PTP1B ASO lowered PTP1B protein (Fig. 1*D*) and mRNA levels (55 ± 8%, *P* < 0.05) in liver of diabetic *db/db* mice treated i.p. weekly for 4 weeks. A UC combinatorial mixture of oligonucleotides (see *Experimental Procedures*) was without effect (Fig. 1*D*) on PTP1B levels in liver.
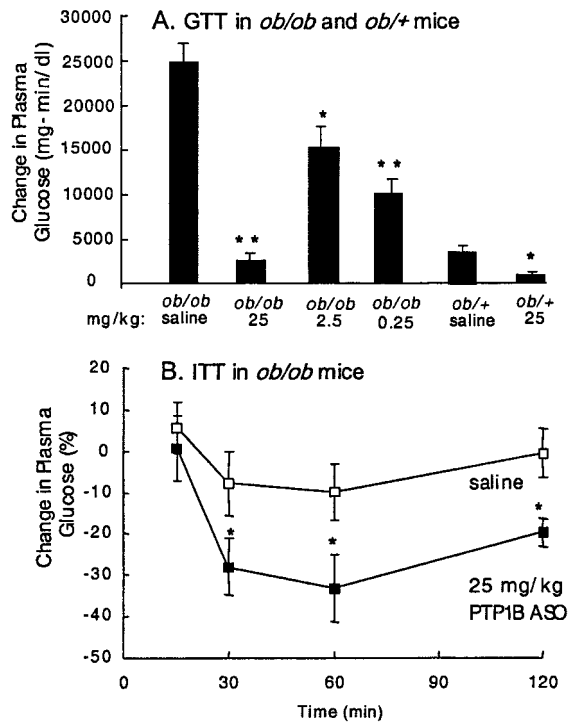
After 2 weeks of treatment, plasma glucose levels in *ob/ob* mice were corrected to lean (*ob/+*) levels in the 25 mg/kg dose group and by week 3 were improved in the 2.5 mg/kg dose group (Fig. 2*A*). After 6 weeks of treatment, an overnight fast reduced glucose levels (30%) in the high-dose group (139 ± 14 vs. 97 ± 3 mg/dl, *P* < 0.05) with no hypoglycemia. HbA$_{1C}$, a measure of long-term glucose homeostasis, was reduced from 6.2 ± 0.3% in saline-treated *ob/ob* mice to 4.7 ± 0.1% (*P* < 0.01) in the 25 mg/kg dose group, a level equivalent to lean *ob/+* littermates (4.8 ± 0.1%). Plasma insulin levels were decreased 77% (Fig. 2*B*) at 6 weeks in the 25 mg/kg-dose group versus the saline-control group. As demonstrated in an i.p. GTT, glucose excursion was corrected to that of lean animals (*ob/+*) in the 25 mg/kg treatment group and improved in the other two dose groups (Fig. 3*A*). Although *ob/+* mice are lean and not diabetic, they are insulin-resistant and have an impaired glucose tolerance compared with wild-type C57BL/6J mice. The PTP1B ASO-treated lean *ob/+* group also had a statistically significant improvement in glucose excursion, with no observed hypoglycemia (Fig. 3*A*). In *ob/ob* mice, an enhanced reduction in glucose level (3.4-fold; Fig. 3*B*) occurred during an ITT with PTP1B ASO treatment. The GTT and ITT results suggest enhanced insulin sensitivity in adipose and liver because PTP1B ASO treatment reduced PTP1B protein levels in liver and adipose tissue with no effect in skeletal muscle. In *db/db* mice, glucose levels were improved in a dose-dependent manner, reaching lean (*db/+*) littermate levels at 50 mg/kg ASO (Fig. 2*C*). No change in plasma glucose in *db/db* mice was observed with 50 mg/kg UC treatment and no effect on glucose level was observed with either PTP1B ASO or UC treatment in *db/+* mice (data not shown). PTP1B ASO treatment was well tolerated in all animals.
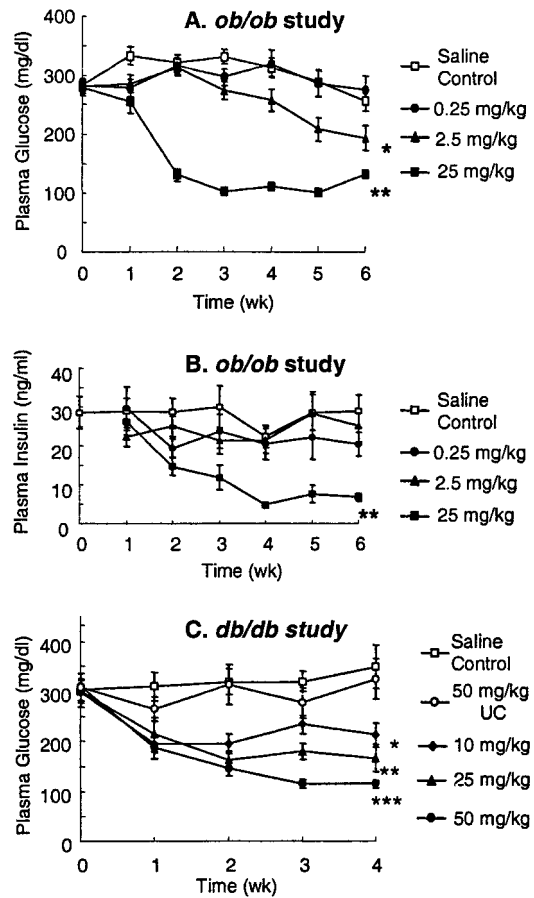
Fig. 2. Non-fasting plasma glucose (*A*) and insulin (*B*) levels versus time in PTP1B ASO-treated *ob/ob* mice (25, 2.5, and 0.25 mg/kg). Nonfasting plasma glucose (*C*) levels versus time in PTP1B ASO-treated *db/db* mice (50, 25, 10, and 50 mg/kg UC). Data are mean ± SE; *, *P* < 0.05; **, *P* < 0.01; ***, *P* < 0.001 (vs. saline control). In *A*, the significance of week 3–6 values dosed at 2.5 mg/kg is *P* < 0.05, and for week 2–6 values dosed at 25 mg/kg is *P* < 0.01. In *B*, the significance of week 3–6 values dosed at 25 mg/kg is *P* < 0.01. In *C*, the significance of week 2–4 values dosed at 10 mg/kg is *P* < 0.05, at 25 mg/kg is *P* < 0.01, and at 50 mg/kg PTP1B ASO is *P* < 0.001.

Molecular toxicology, blood chemistry, and histological examination indicated that PTP1B ASO treatment at these doses did not adversely affect liver function or the general health of the *ob/ob* mice in these studies.

Non-fasted body weights were not different between saline-control and ASO treatment at 0.25, 2.5, and 25 mg/kg over the duration of the 6-week study (Table 1). Weekly weight gain was not different between treatments (data not shown). Epididymal fat weight was reduced 42% with high-dose treatment (*P* < 0.05, normalized to brain weight) and unchanged with lower dose treatments versus saline control (Table 1). Liver weight was increased 36% with 25 mg/kg PTP1B ASO treatment only (*P* < 0.05, normalized to brain weight; Table 1). It is possible that metabolism of lipids was altered such that flux through utilization pathways (and/or diminished storage) was enhanced resulting in reduced fat weight. Future studies are needed to determine the meaning and mechanism of this observation in this model. Estimated food consumption was decreased in the 25 mg/kg PTP1B ASO-treated *ob/ob* mice compared with the saline controls during week 6 (4.9 ± 0.3 vs. 5.9 ± 0.3 g/day; *P* < 0.05; 25 mg/kg PTP1B ASO versus saline). There were no differences in food intake during weeks 1, 2, and 5 (*P* > 0.05). Consequently, reduction in weight gain and food intake is

Fig. 3. PTP1B ASO treatment increases insulin sensitivity in *ob/ob* mice. (*A*) Change in AUC (area under the curve) for plasma glucose after an i.p. GTT. (*B*) Change in plasma glucose level after an ITT in *ob/ob* mice. Results are expressed as change from baseline AUC_Glucose for GTT (25, 2.5, and 0.25 mg/kg PTP1B ASO treatment in *ob/ob* and 25 mg/kg PTP1B ASO treatment in lean littermates, *ob/+*). Results are expressed as percentage change from baseline for ITT. GTT and ITT were performed in week 6 of treatment. Data are mean ± SE; ∗, $P < 0.05$; ∗∗, $P < 0.01$; ∗∗∗, $P < 0.001$ (vs. saline control).

Fig. 4. PTP1B ASO treatment affects the level of IRS-2 and PI3-kinase regulatory subunit (p85α and p50α) expression in *ob/ob* mouse liver and fat. Representative immunoblots using anti-IRS-2 antibodies (*A* and *B*) or anti-p85α whole antiserum that recognized all p85 isoforms (*C–F*) were quantified. The results are the average of four mice within each group. The data are represented as arbitrary units and are the mean ± SEM. Statistics were determined as a two-tailed *t* test. ∗, $P < 0.05$; ∗∗, $P < 0.01$; ∗∗∗, $P < 0.001$ (vs. saline control).
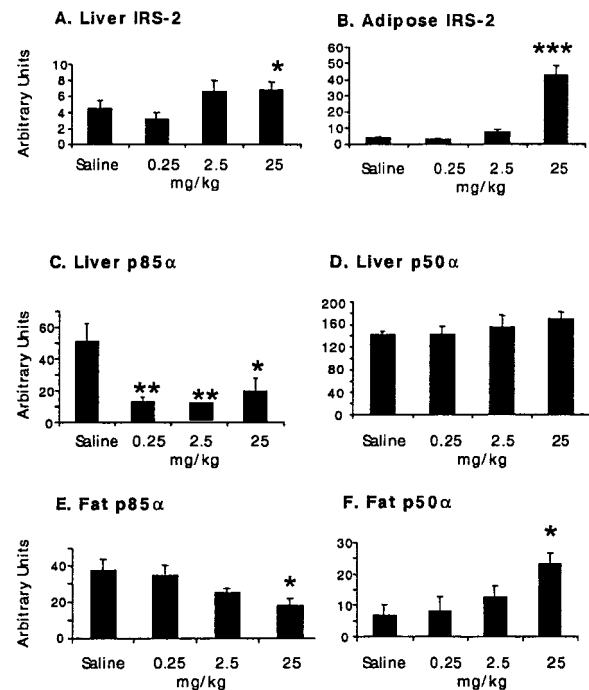
unlikely to be responsible for the normalization of glucose and the decrease in insulin levels. Examination of the *ob/ob* mice in these studies for changes in histopathology, blood chemistry, and molecular toxicology did not reveal any adverse reaction to treatment with the PTP1B ASO.

Stimulation of IR kinase activity (19, 20) induces the tyrosine phosphorylation of endogenous substrates including IRS-1 to -4 (9). IRS proteins interact with and recruit SH2 domain-containing proteins, including phosphatidylinositol 3 (PI3-kinase; refs. 21 and 22). In *ob/ob* diabetic mice, the expression levels of IR, IRS-1, and IRS-2 are reduced relative to lean littermates, and may contribute to the insulin-resistant phenotype (23). Although in gene deletion experiments PTP1B has been shown to be an important regulator of IR and IRS-1 in

Table 1. Body, epididymal fat, and liver weights (g) after 6 weeks of saline or PTP1B antisense treatment (2qw, i.p.) in nonfasted *ob/ob* mice

|	Body weight	Epididymal fat	Liver
Saline	58.1 ± 1.3	4.9 ± 0.1	4.0 ± 0.1
0.25 mg/kg	59.1 ± 0.8	5.0 ± 0.3	3.6 ± 0.2
2.5 mg/kg	59.3 ± 1.4	4.2 ± 0.3	4.5 ± 0.2
25 mg/kg	56.4 ± 1.1	3.0 ± 0.2∗∗∗	5.6 ± 0.3∗∗

Data are mean ± SE. Epididymal fat and liver weights were normalized to brain weight for each animal for statistical purposes. There were no differences between treatments in brain weight ($P > 0.05$). ∗∗, $P < 0.01$; ∗∗∗, $P < 0.001$ vs. saline control. At randomization on day 1, body weights did not differ between groups (37.1 ± 0.6, 37.6 ± 0.8, 37.5 ± 0.8, and 37.2 ± 0.7 g; saline control, 0.25, 2.5, and 25 mg/kg PTP1B ASO treatment, respectively).

nondiabetic mice (13, 14), it is not clear that a decrease in PTP1B expression will regulate proteins involved in the insulin-signaling pathway in the diabetic state. We therefore measured the protein expression of IR, IRS-1, IRS-2, and PI3-kinase isoforms in liver and fat from *ob/ob* and *ob/+* mice treated with PTP1B ASO by immunoblotting. No effect on IR or IRS-1 expression was detected in liver or fat (data not shown) from PTP1B-ASO treated mice, although reduced expression of IR, IRS-1, and IRS-2 was confirmed in *ob/ob* relative to *ob/+* mice, as reported (23). Reduced levels of IRS-2, considered important in hepatic insulin signal transduction (24), could contribute to hepatic insulin resistance and increased IRS-2 expression could improve hepatic insulin sensitivity. Although a direct causality cannot be established, IRS-2 protein levels were increased in a dose-dependent manner in liver and fat in *ob/ob* mice treated for 6 weeks with PTP1B ASO (Fig. 4 *A* and *B*). PTP1B ASO treatment had no effect on IRS-2 levels in the same tissues from lean *ob/+* mice (data not shown).

IRS-1 and IRS-2 link IR to its final actions through a series of intermediate effectors. One of the key enzymes downstream of metabolic IR signaling is PI3-kinase (21, 22, 25). PI3-kinase is a heterodimeric enzyme composed of a regulatory subunit (p85α) and a catalytic subunit (p110). Additional isoforms of p85α (e.g., p55α and p50α) have also been described (25). Mice with targeted disruption of the gene encoding the p85α subunit of PI3-kinase have increased levels of p55α and p50α, and exhibit increased insulin sensitivity and hypoglycemia (26). The change in isoform expression is associated with increased insulin-induced phosphatidylinositol 3,4,5-triphosphate formation, increased GLUT4 translocation, and increased glucose transport into fat and muscle. To determine whether insulin sensitization was associated with a change in PI3-kinase expression, homog-

A) IP: anti-PY

Blot: anti-PY   Blot: Anti-IR

B) Blot: anti-pPKB (thr ³⁰⁸)
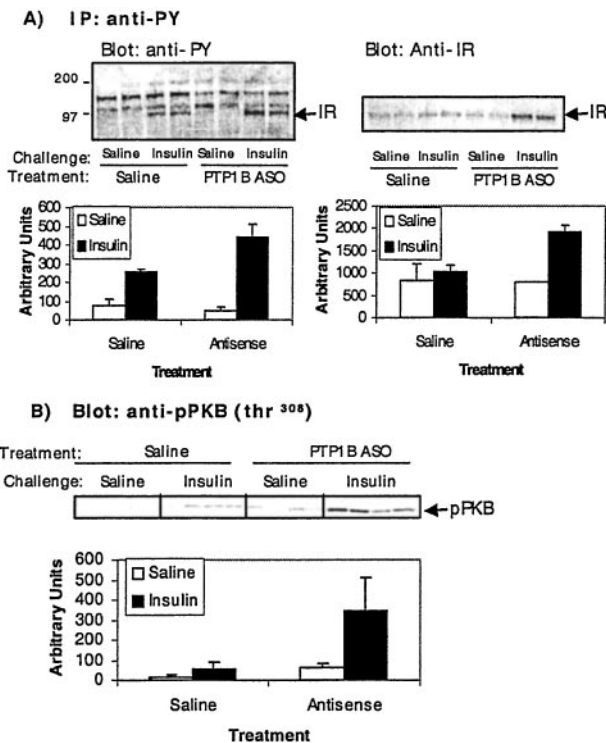
Fig. 5. PTP1B ASO causes enhanced insulin signaling in liver. PTP1B ASO (25 mg/kg, i.p. dosed twice per week for 6 weeks) or saline-treated *ob/ob* mice were fasted for 5 h and then challenged with an i.p. bolus of saline or insulin (2 units/kg in 0.1% BSA). Liver tissue was taken at 1 min following saline or insulin challenge. (*A*) Cell lysates were immunoprecipitated using anti-phosphotyrosine (PY) antibodies and immunoblotted with anti-PY and anti-IR antibodies as indicated. (*B*) Cell lysates were loaded by equal amount of proteins, separated by SDS/PAGE (7.5% gels), and immunoblotted with anti-phosphothreonine-308-specific PKB antibodies.

enates of liver and fat from PTP1B ASO-treated lean and obese animals were immunoblotted with p85α antiserum. A dose-dependent reduction of p85α isoform expression in both liver and fat was observed along with increased expression of the p50α isoform in fat (Fig. 4). In a 3-week study in *ob/ob* mice dosed at 50 mg/kg i.p., twice per week with PTP1B ASO, a similar phenotype was observed with decreased expression of p85α in liver (40%, $P < 0.04$) and fat (30%, $P < 0.01$). In the same study, increased expression of both p50α, 2-fold in liver ($P < 0.01$) and 20-fold in fat ($P < 0.01$), and p55α, 6-fold in liver ($P < 0.01$), was observed (data not shown). No changes in PI3-kinase isoform expression were observed in skeletal muscle, supporting the notion that the changes were not secondary to a generalized improvement in glucose tolerance and insulin sensitivity (data not shown). Differential expression of PI3-kinase regulatory subunits observed in the PTP1B ASO-treated *ob/ob* mice would be predicted to increase insulin sensitivity in liver and fat and is consistent with the improved glucose tolerance observed in these diabetic mice.

To determine whether PTP1B ASO enhanced insulin signaling we investigated the effect of the PTP1B ASO treatment on insulin-dependent IR tyrosine phosphorylation (Fig. 5*A*). An i.p. insulin challenge (2 units/kg) was performed in *ob/ob* mice previously treated for 6 weeks with saline or 25 mg/kg PTP1B ASO. Livers were extracted at 1 min post insulin or saline challenge. An approximate 2-fold increase in the insulin-dependent tyrosine phosphorylation of the insulin receptor was observed in the PTP1B ASO-treatment animals compared with saline-treated animals. PKB is thought to regulate some IR metabolic responses downstream of IRS and PI3-kinase (27, 28). Treatment with PTP1B ASO slightly increased basal PKB phosphothreonine-308 levels. However, ASO treatment caused a much greater enhancement ($\approx$4-fold) in insulin-stimulated PKB Thr-308 phosphorylation (Fig. 5*B*). PKB protein levels were unchanged by PTP1B ASO treatment (data not shown). The increased phosphorylation of PKB is further evidence of increased insulin sensitivity in the liver as a result of PTP1B ASO treatment, and correlates with changes in the expression of insulin signaling proteins IRS-2 and PI3-kinase isoforms.

Hepatic glucose production has a prominent role in systemic glucose homeostasis. Insulin decreases hepatic glucose output by activating glycogen synthesis and glycolysis and by inhibiting gluconeogenesis. Several reports have suggested that PKB is a regulator of gluconeogenesis and glycogen synthesis in liver (29–32). Insulin regulates glycogen synthesis and glycolysis presumably through a PI3-kinase-dependent pathway (21). Insulin also inhibits glucagon and glucocorticoid-induced phosphoenolpyruvate carboxykinase (PEPCK) expression acting through PI3-kinase (33, 34). PEPCK is a rate-limiting step in hepatic gluconeogenesis that is regulated at the transcription level and fructose-1,6-bisphosphatase (F-1,6-BP) is also a key enzyme in this pathway. To investigate the effect of reduced PTP1B protein levels on these downstream events in the hepatic insulin signaling pathway, we measured mRNA levels by microarray analysis (Affymetrix murine 11K chip) comparing PTP1B ASO-treated to saline-treated diabetic *ob/ob* mice. PTP1B ASO significantly reduced PEPCK mRNA levels (38%) and F-1,6-BP (17%) in *ob/ob* mice treated for 6 weeks at 25 mg/kg. A similar reduction was observed for both PEPCK (55%) and F-1,6-BP (52%) mRNA in an independent *ob/ob* mouse study dosing i.p. twice per week for 3 weeks with 50 mg/kg PTP1B ASO.

Reduction of PTP1B protein levels in the diabetic state by using the PTP1B ASO positively modulates insulin-signaling proteins in liver and fat. Increased insulin sensitivity and PKB activation in liver could cause the observed decrease in PEPCK mRNA levels and associated decrease in hepatic glucose output. Decreased hepatic glucose output, as well as a putative increase in insulin sensitivity in fat, could account for the observed improvement in glucose control in PTP1B ASO-treated *ob/ob* mice. These results suggest that a relative over-activity of PTP1B is important to the maintenance of the diabetic state and that inhibition of PTP1B activity, as with a PTP1B ASO-induced decrease in PTP1B protein expression, may provide therapeutic benefit for the treatment of type 2 diabetes.

1. Reaven, G. M. (1988) *Diabetes* **37,** 1595–1607.
2. Olefsky, J. M., Garvey, W. T., Henry, R. R., Brillon, D., Matthai, S. & Friedenberg, G. R. (1988) *Am. J. Med.* **85,** Suppl. 5A, 86–105.
3. Kruszynska, Y. T. & Olefsky, J. M. (1996) *J. Invest. Med.* **44,** 413–428.
4. Youngren, J. F. & Goldfine, I. D. (1997) *Sci. Med.* **4,** 18–27.
5. Kahn, C. R. (1994) *Diabetes* **43,** 1066–1084.
6. Czech, M. P. & Corvera, S. (1999) *J. Biol. Chem.* **274,** 1865–1868.
7. Kao, A. W., Waters, S. B., Okada, S. & Pessin, J. E. (1997) *Endocrinology* **138,** 2474–2480.
8. Olefsky, J. M. (1999) *J. Biol. Chem.* **274,** 1863.
9. White, M. F. (1998) *Mol. Cell. Biochem.* **182,** 3–11.
10. Kenner, K. A., Anyanwu, E., Olefsky, J. M. & Kusari, J. (1996) *J. Biol. Chem.* **271,** 19810–19819.
11. Kennedy, B. P. & Ramachandran, C. (2000) *Mol. Pharmacol.* **60,** 877–883.

MEDICAL SCIENCES

12. Goldstein, B. J., Bittner-Kowalczyk, A., White, M. F. & Harbeck, M. (2000) *J. Biol. Chem.* **275,** 4283–4289.

13. Klaman, L. D., Boss, O., Peroni, O. D., Kim, J. K., Martino, J. L., Zabolotony, J. M., Moghal, N., Lubkin, M., Kim, Y.-B., Sharpe, A. H., *et al.* (2000) *Mol. Cell. Biol.* **20,** 5479–5489.

14. Elchebly, M., Payette, P., Michaliszyn, E., Cromlish, W., Collins, S., Loy, A. L., Normandin, D., Cheng, A., Himms-Hagen, J., Chan, C. C., *et al.* (1999) *Science* **283,** 1544–1548.

15. Baker, B. F. & Monia, B. P. (1999) *Biochim. Biophys. Acta* **1489,** 3–18.

16. Crooke, S. T. & Bennett, C. F. (1996) *Annu. Rev. Pharmacol. Toxicol.* **36,** 107–129.

17. Dean, N. M., Butler, M., Monia, B. P. & Manoharan, M. (2001) in *Antisense Drug Technology: Principles, Strategies and Applications*, ed. Crooke, S. T. (Dekker, New York), pp. 319–338.

18. Levin, A. A. (1999) *Biochim. Biophys. Acta* **1489,** 69–84.

19. Kasuga, M., Fujita-Yamaguchi, Y., Blithe, D. L. & Kahn, C. R. (1983) *Proc. Natl. Acad. Sci. USA* **8,** 2137–2141.

20. Herrera, R. & Rosen, O. M. (1986) *J. Biol. Chem.* **261,** 11980–11985.

21. Ruderman, N. B., Kapeller, R., White, M. F. & Cantley, L. C. (1990) *Proc. Natl. Acad. Sci. USA* **87,** 1411–1415.

22. Cheatham, B., Vlahos, C. J., Cheatham, L., Wang, L., Blenis, J. & Kahn, C. R. (1994) *Mol. Cell. Biol.* **14,** 4902–4911.

23. Kerouz, N. J., Horsch, D., Pons, S. & Kahn, C. R. (1997) *J. Clin. Invest.* **100,** 3164–3172.

24. Kido, Y., Burks, D. J., Withers, D., Bruning, J. C., Kahn, C. R., White, M. F. & Accilli, D. (2000) *J. Clin. Invest.* **105,** 199–205.

25. Inukai, K., Funaki, M., Ogihara, T., Katagiri, H., Kanda, A., Anai, M., Fukushima, Y., Hosaka, T., Suzuki, M., Shin, B. C., *et al.* (1997) *J. Biol. Chem.* **272,** 7873–7882.

26. Terauchi, Y., Tsuji, Y., Satoh, S., Minoura, H., Murakami, K., Okuno, A., Inukai, K., Asano, T., Kaburagi, Y., Ueki, K., *et al.* (1999) *Nat. Genet.* **21,** 230–235.

27. Alessi, D. R., Andjelkovic, M., Caudwell, B., Cron, P., Morrice, N., Cohen, P. & Hemmings, B. A. (1996) *EMBO J.* **15,** 6541–6551.

28. Alessi, D. R. & Cohen, P. (1998) *Curr. Opin. Genet. Dev.* **8,** 55–62.

29. Deprez, J., Vertommen, D., Alessi, D. R., Hue, L. & Rider, M. H. (1997) *J. Biol. Chem.* **272,** 17269–17275.

30. Lefebvre, V., Mechin, M. C., Louckx, M. P., Rider, M. H. & Hue, L. (1996) *J. Biol. Chem.* **271,** 22289–22292.

31. Peak, M., Rochford, J. J., Borthwick, A. C., Yeaman, S. J. & Agius, L. (1998) *Diabetologia* **41,** 16–25.

32. Liao, J., Barthel, A., Nakatani, K. & Roth, R. A. (1998) *J. Biol. Chem.* **273,** 27320–27324.

33. Gabbay, R. A., Sutherland, C., Gnudi, L., Kahn, B. B., O'Brien, R. M., Granner, D. K. & Flier, J. S. (1996) *J. Biol. Chem.* **271,** 1890–1897.

34. Sutherland, C., O'Brien, R. M. & Granner, D. K. (1995) *J. Biol. Chem.* **270,** 15501–15506.